Anomalous Difference in the Order−Disorder Transition Temperature Comparing a Symmetric Diblock Copolymer AB with Its Hetero-Four-Arm Star Analog A_2B_2

D. M. A. Buzza,*,†,‡ I. W. Hamley,§ A. H. Fzea,∥,⊥ M. Moniruzzaman,∥ J. B. Allgaier,∥ R. N. Young,∥ P. D. Olmsted,† and T. C. B. McLeish†

Department of Physics and Astronomy and Polymer IRC, University of Leeds, Leeds LS2 9JT, U.K., School of Chemistry, University of Leeds, Leeds LS2 9JT, U.K., and Department of Chemistry, University of Sheffield, Sheffield S3 7HF, U.K.

Received March 18, 1999; Revised Manuscript Received June 28, 1999

ABSTRACT: The order−disorder transition temperature (T_{ODT}) of symmetric styrene−isoprene diblock copolymers (AB) and its hetero-four-arm star analog (A_2B_2) was measured using dynamic mechanical spectroscopy and small-angle X-ray scattering (SAXS). Care was taken to ensure that the arm molecular weights of both AB and A_2B_2 were matched. Contrary to mean-field theory predictions, a significant difference in T_{ODT}, $\Delta T_{ODT} \approx 30$ °C, is found between the two systems (the arm molecular weight for both the styrene and isoprene is about 10 kg mol^{-1}). We show that this difference is too large to be explained by polydispersity, segmental asymmetry, or the Fredrickson−Helfand theory of compositional fluctuations (which assumes that the polymer chains are Gaussian). Instead, we suggest that one needs to incorporate the differing degrees of non-Gaussian chain stretching in the two systems at the order−disorder transition (as confirmed by SAXS) into the fluctuation theory for a proper understanding of the effect. We demonstrate that a simple model calculation that incorporates sufficient chain stretching to match the experimentally determined shifts in the SAXS peak for the two systems also reproduces a difference in the T_{ODT} which is comparable to what is measured experimentally.

I. Introduction

Block copolymers are macromolecules where sequences, or blocks, of chemically distinct repeat units are covalently bonded together within the same molecule. One of the most striking features of these macromolecules is that in the melt phase, the distinct chemical units microphase separate at low enough temperatures to form ordered microdomains whose length scale is of the order of the the size of a molecule. This transition is called the order−disorder transition (ODT), and the temperature at which it occurs is known as the order-disorder transition temperature (T_{ODT}). Until relatively recently, most of the the experimental and theoretical work on block copolymers has tended to focus on the simplest block copolymers, i.e. AB diblock copolymers. However, advances in synthetic chemistry, especially in the area of anionic polymerization, have allowed block copolymers with more complex molecular architectures to be synthesized, opening up a whole new dimension in block copolymer research, namely the influence of molecular architecture and topology on solution and melt properties of block copolymers. In this study, the specific architecture we shall consider is that of heteroarm star block copolymers of the A_nB_n type, i.e., where n A blocks and n B blocks are covalently bonded at a single point to form a star-shaped molecule (see Figure 1). Block copolymers with this architecture have been successfully synthesized by various co-workers using anionic polymerization.[1−4]

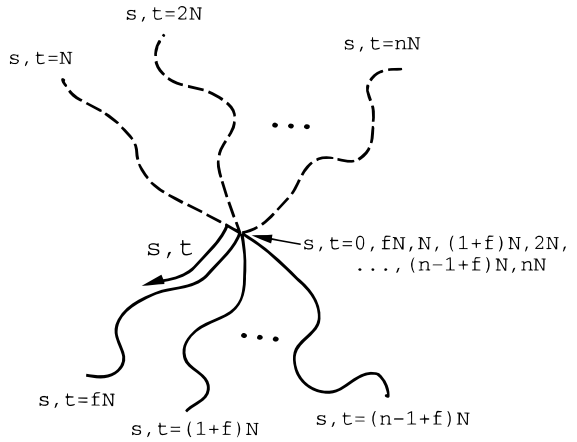

Figure 1. A_nB_n polymer and the definition of monomer indices.

The position of the ODT for A_nB_n (assuming equal segmental lengths and volumes for A and B monomers) was calculated using mean-field theory (or random phase approximation, RPA) by Olvera de la Cruz and Sanchez.[5] They found the surprising result that for symmetric A_nB_n, where each A and B arm consists of $N/2$ monomers, the ODT occurs at

$$(\chi N)_{ODT} = 10.495 \qquad (1)$$

for all values of n, where χ is the Flory interaction parameter between the A and B monomers; this means that the T_{ODT} is identical for all A_nB_n independent of n. In order to test this prediction of the mean-field theory, we have synthesized, using anionic polymerization, symmetric styrene−isoprene diblock copolymers AB ($n = 1$) together with their A_2B_2 analog ($n = 2$), i.e., where the A_2B_2 can be thought of as being due to two AB

† Department of Physics and Astronomy and Polymer IRC, University of Leeds.
‡ E-mail: d.m.a.buzza@leeds.ac.uk.
§ School of Chemistry, University of Leeds.
∥ Department of Chemistry, University of Sheffield.
⊥ Present address: Department of Chemistry, University of Dundee, Dundee DD1 4HN, U.K.

10.1021/ma9904060 CCC: $18.00
Published on Web 10/12/1999

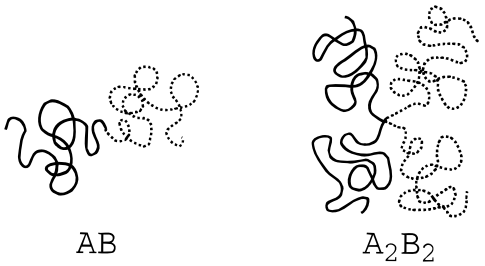

Figure 2. AB diblock and A_2B_2 hetero-four-arm star.

diblocks joined together at their block junctions (see Figure 2). The advantage of anionic polymerization is that it allows us to produce block copolymers with a well-defined architecture and very narrow molecular weight distribution. This in turn allows for a stringent experimental test of the mean-field theory prediction. Measuring their respective T_{ODT}s, we find, in contrast to mean-field theory predictions, significant differences between AB and A_2B_2 (section III).

One obvious explanation for this is the fact that, in mean-field theory, compositional fluctuations about the mean compositional profile have been neglected. Previous theoretical and experimental studies have shown that these fluctuations become important for symmetric block copolymers near the ODT[6−10] and that they qualitatively modify the RPA predictions. For symmetric diblocks, the ODT is predicted to be first order rather than second order and occurs at a higher value of (χN) (i.e., lower value of T_{ODT}) than that predicted by RPA.[6,9,10] In addition, fluctuations induce chain stretching so that the individual chain statistics are no longer Gaussian (i.e., the radius of gyration $R_g \sim N^{\delta}$ with $\delta > {}^1/_2$),[7−10] as assumed in RPA. In subsection VA, we show that the simplest fluctuation theory which assumes that the block copolymer chains remain Gaussian[6] cannot fully account for the difference in T_{ODT}. Instead, we suggest that one needs to incorporate the more subtle effect of non-Gaussian stretching into the fluctuation calculation in order to explain the experimental result.

We should mention here that there have been some recent studies by Beyer et al.[11] and Turner et al.[12] comparing the properties of nearly symmetric AB diblocks with A_nB_n block copolymers ($n = 8$ in ref 11 and $n = 2$ in ref 12). In particular, Turner et al. have compared nearly symmetric AB diblocks with their A_2B_2 analogs. By measuring the lamellar domain spacing in these systems using transmission electron microscopy (TEM) and small-angle X-ray scattering (SAXS), both groups find that the dimensionless area per molecule normalized for total molecular weight $AN_{total}^{2/3}/R_g^2$ scales as n^{δ}, with $\delta \approx 1$. Here A is the area per molecule (derived from the domain spacing), N_{total} is the total number of monomers in A_nB_n, and R_g is the theoretically calculated value of the radius of gyration (corrected for crowding effects for A_8B_8 in ref 11). The present work differs from both these studies in two important respects. First, the block copolymer samples in refs 11 and 12 were studied well below the T_{ODT} so that the strong or intermediate segregation regime applies while, in this study, we are specifically interested in the material properties at or near the ODT where weak segregation applies. Our work therefore differs qualitatively from and complements that of refs 11 and 12, giving us a better understanding of these systems over the whole range of χN values. Second, in order to test the predictions of eq 1 stringently, great care was taken in the synthesis step to ensure that the arm molecular weights for both AB and A_2B_2 were identically matched (section IIA). This allows us to directly compare the T_{ODT} results of AB and A_2B_2 with each other and to the theory without further corrections for discrepancies in molecular weights. Interestingly, our measurements of the domain spacings in the weakly ordered regime turn out to be consistent with the measurements of Turner et al. in the well-ordered regime; namely, the domain spacing for A_2B_2 stars is found to be greater than that of their linear AB analogs (see subsection IIIB). This fact will be of crucial importance in section V where we use a simple model calculation due to Maurer et al.[13] to explain the observed discrepancy in the T_{ODT} between linears and stars.

The rest of this paper is organized as follows. In section II we give details of the synthesis and characterization of the AB and A_2B_2 block copolymers as well as the experimental techniques used to measure T_{ODT}, namely rheology and SAXS. In section III, results for both T_{ODT} and q^* (the principle scattering peak) are presented. In section IV, the mean-field calculation of $(\chi N)_{ODT}$ is presented for the case of segmentally symmetric monomers (subsection IVA) and segmentally asymmetric monomers (subsection IVB); we show that neither version of the mean-field theory is capable of explaining the large discrepancy in T_{ODT} between AB and A_2B_2 found experimentally. In section V, we show that a naive consideration of compositional fluctuations which neglects non-Gaussian stretching cannot fully account for the experimental data. Instead, we present a simple model calculation which incorporates non-Gaussian stretching into the fluctuation theory and show that this gives us differences in the T_{ODT} which are comparable to experiments. Finally, section VI is our conclusion.

II. Experimental Section

A. Synthesis of Styrene Isoprene AB and A_2B_2 Block Copolymers. High-vacuum techniques, all-glass reactors, and break-seal procedures were used throughout. Styrene was distilled on to dibutylmagnesium and allowed to stand for several hours before being distilled into a reactor. Isoprene was treated similarly but was additionally stored over *n*-butyllithium for 20 min at −10 to −20 °C. Small quantites of butadiene were similarly purified and transferred into ampules. Benzene, cyclohexane, and triethylamine were all distilled from solutions of polystyryllithium. *s*-Butyllithium was purified by distillation on to a cold finger in a short path length apparatus, dissolved in cyclohexane, and ampulized. Silicon tetrachloride was distilled on the vacuum line: after the discard of some 30% of the original volume, the next 30% was collected, diluted with cyclohexane, and ampulized. Dimethyldichlorosilane (Me_2SiCl_2) was treated similarly.

The A_2B_2 heteroarm stars were synthesized as follows. Styrene was polymerized in benzene using *s*-BuLi as initiator. After 24 h a small sample was isolated in a side arm for subsequent SEC analysis. $SiCl_4$ was introduced into the reactor such that the ratio [$SiCl_4$]:[Li] was 1:2.04, and reaction was allowed to proceed for 1 day whereupon a sample was again removed for analysis. Due to the bulky nature of polystyrene, steric hindrance ensures that the living polystyrene reacts with just two chlorine atoms of $SiCl_4$. This is confirmed by characterization of the reaction products using SEC which shows that $(PS)_2SiCl_2$ is formed unaccompanied by $(PS)_3SiCl$ or $(PS)_4Si$ (see Figure 3 and accompanying text). A small peak representing the molecular weight of a single PS block was also seen in the SEC trace (not shown in Figure 3); this corresponds to unreacted living PS blocks due to the small stoichiometric excess of living PS. The fact that the peak is due to living PS

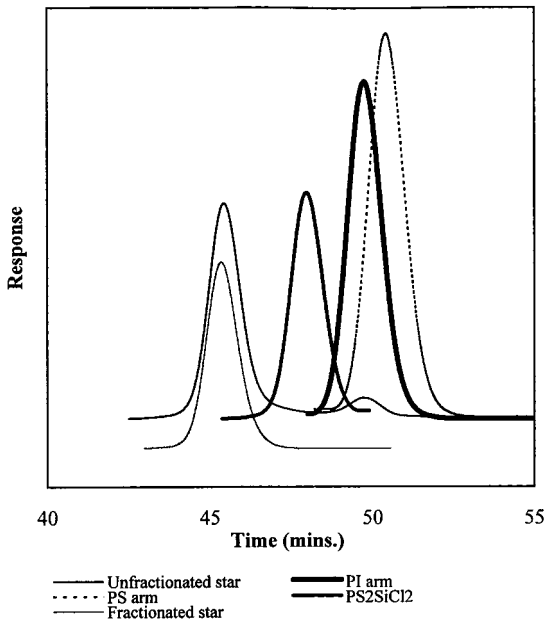

Figure 3. SEC traces at different stages in the synthesis of m-A_2B_2.

rather than $(PS)SiCl_3$ is confirmed by measuring the weight percent of PS in the final A_2B_2 product using ^{1}H NMR; a PS weight percent close to 50% was found, as expected for pure A_2B_2 (see Table 1). The bulky nature of PS was similarly exploited by Hadjichristidis and co-workers in synthesizing polystyrene−polybutadiene A_2B_2 heteroarm (or miktoarm) star block copolymers[1] and $(PS-PI)_2$-$(PS-PI)_2$ star block copolymers.[14]

Isoprene was similarly polymerized in a separate reactor using sufficient benzene to keep the [*s*-BuLi] below 5×10^{-3} molar so as to ensure a high content of 1,4-enchainment. After 1 day, the living polyisoprene was capped with about 5 units of butadiene; a sample of the polydiene was isolated for SEC analysis. The two reactors were fused together, and the living polydiene was transferred into the styrene vessel via a break-seal. The quantities of the two polymer solutions were programmed to have about 2.3 equiv of polydienyllithium to each atom of silicon. After the samples reacted for 2 days, a few milliliters of triethylamine were added to facilitate completion of the coupling reaction. Methanol was added after a further 3 or 4 days, and the polymer was isolated.

The AB diblock copolymer was prepared in the conventional manner in a single reactor by first polymerizing styrene and then introducing the isoprene monomer to the living polystyrene.

To create a perfectly matched AB and A_2B_2 pair having *identical* A and B blocks, large batches of living polystyrene and polyisoprene were prepared in graduated reaction flasks. Half of each of these solutions was used to prepare the star as described above. The other halves were converted into an AB diblock as follows: the polystyryllithium solution was cooled to 5 °C, and a 20-fold excess of Me_2SiCl_2 was added to it. The reaction was then allowed to proceed for 12 h at ambient temperature. Unreacted Me_2SiCl_2 and the benzene solvent were removed by distillation under vacuum. The residue was dissolved in fresh benzene which was once again removed and pumping was continued overnight; this sequence was repeated to ensure that no Me_2SiCl_2 remained. Analysis of a small sample showed that no chain coupling had occurred. The solution of butadiene-capped polyisoprenyllithium was introduced at a level of 10% in excess of that required for stoichiometric equivalence, and reaction was allowed to proceed for 2 days. Pure star and diblock were obtained by fractional precipitation from a toluene/petroleum solution using methanol.

B. Characterization. Size exclusion chromotography (SEC) analysis was with THF solutions at a flow rate of 1 mL min^{-1}. Separation was either by four linear Phenomenex columns together with a RI detector or by six linear Ultrastyragel columns with triple detector (RI, viscosity, and light scattering) and calibration was with polystyrene and polyisoprene standards. Weight average molecular weights were determined by low-angle laser light scattering at 25 °C with a Chromatix KMX-6 LALLS photometer operating at 633 nm. The solvent was THF. The d*n*/d*c* values were measured in THF at 25 °C with a Chromatix KMX-16 differential refractometer operating at 633 nm and calibrated with NaCl solutions. The compositions of all copolymers were determined by ^{1}H NMR spectroscopy using a Bruker AC250 instrument.

The course of the synthesis of the A_2B_2 stars was monitored by SEC as shown in Figure 3. The trace for the parent PS arm shows a large sharp peak at 50.5 min, and that for the parent PI, at 49.8 min, both ams having a low dispersity (Table 1). The trace for the product of the reaction of the PSLi with $SiCl_4$ has a sharp peak at 48.0 min representing substitution of solely two chlorine atoms of $SiCl_4$ to form $(PS)_2SiCl_2$ with dispersity 1.02. Preliminary experiments had shown that the reaction of PILi with $(PS)_2SiCl_2$ virtually stops when the three armed star is formed—presumably because of steric hindrance. For that reason the PILi was end capped with a few units of butadiene as the PBLi chain end is sterically less hindered. Even so, SEC analysis showed that after 1 day only one of the remaining chlorine atoms had been replaced forming a three-armed star. After reaction for 2 days, triethylamine was introduced to facilitate the linking reaction, and after a further 3 or 4 days the reaction was terminated with methanol and the product recovered. SEC analysis showed the linking had gone to completion with the elution peak of the 4-armed star at 45.5 min together with a small peak at 49.8 min representing the excess PI arm. Fractionation removed the latter yielding pure A_2B_2 star with a low dispersity (1.01).

Limiting the reaction of polystyryllithium with Me_2SiCl_2 to the formation only of $(St)Me_2SiCl$ was achieved by using a very large excess of Me_2SiCl_2. The initial mixing was conducted at a somewhat reduced temperature to minimize the possibility of coupling arising from momentary local high concentrations of living chains during the actual dispersion of the solutions in each other. SEC confirmed the absence of linked polymer. After removal of the excess Me_2SiCl_2 by prolonged evacuation, reaction with an excess of PILi readily led to the formation of the diblock. Pure material was obtained by fractionation.

The molecular weight and dispersity data are collected in Table 1. The AB and A_2B_2 copolymers designated "u" were prepared quite separately. A target molecular weight was set at 10 000 for each block, and it can be seen that this was met quite successfully. However, in order to have an AB and A_2B_2 pair which had truly identical block lengths it is necessary to assemble these from the same stocks of unlinked parent living

Table 1. Molecular Weight and Dispersity Data for Styrene−Isoprene Block Copolymers

	styrene arm		isoprene arm		copolymer		% styrene (w/w)	
sample[a]	M_n/g mol^{-1}	M_w/M_n	M_n/g mol^{-1}	M_w/M_n	M_n/g mol^{-1}	M_w/M_n	SEC	NMR
u-AB	10 300[b]	1.02[b]	10 800[b]		21 100[b]	1.01[b]	49	48
u-A_2B_2	10 300[b]	1.02[b]	9 700[b]	1.02[b]	40 000[c]	1.01[b]	52	49
m-AB	11 500[d]	1.02[d]	9 840[d]	1.02[d]	22 200[d]	1.01[d]	54	51
m-A_2B_2	11 500[d]	1.02[d]	9 840[d]	1.02[d]	43 800[d]	1.01[d]	54	51

[a] Prefix u samples prepared totally independently of each other; prefix m samples prepared from the same parent arm batches. [b] Determined by SEC with RI detector. [c] M_w determined by static light scattering. [d] Determined by SEC with triple detector.

polymer arms. Confirmation that this had been successful was provided by independent analysis by SEC using a light scattering, viscosity, and refractive index detector which shows that the molecular weights of the copolymers are in good agreement with expectation based on the molecular weights of the constituent blocks. In addition, ^{1}H NMR spectroscopy shows that the proportions of the two monomers in the two copolymers are identical.

C. Rheology. Rheological measurements were performed using a Rheometrics RDA2 rheometer comprising a 25 mm diameter parallel plate geometry. The block copolymer samples were prepared for rheology measurements as follows: An amount of bulk polymer (approximately 1 g) was made into a disk by compression (using a pressing device) at room temperature. The disk was then transferred into a vacuum oven and annealed at 120 °C for 24 h. After being cooled to room temperature, the disk was placed in the rheometer oven and heated to 120 °C under nitrogen gas atmosphere for 1 h to remove any air bubbles prior to any rheology tests. The disk was then pressed between the rheometer plates at 120 °C until a diameter of 25 mm and a thickness of approximately 1.5 mm were obtained. After cooling of the samples to room temperature, the oven door was opened and any excess material around the plates was removed by a sharp razor blade. The oven was closed again, and the temperature was increased to 100 °C; this was maintained for 30 min with enough normal force applied on the plates for the polymer to conform to the plate diameter.

To determine T_{ODT}, we performed dynamic temperature sweeps with temperatures decreasing or increasing at a rate of 5 °C/min. A strain amplitude of 5% at a frequency of 10 rad/s was applied to the sample during cooling or heating. According to well-documented procedures[15,16] the order−disorder transition (ODT) can be identified by a sharp drop in the storage modulus (G') on heating or a sharp rise in G' on cooling.

D. Small-Angle X-ray Scattering. SAXS experiments were conducted at the Synchrotron Radiation Source, Daresbury Laboratory, Daresbury, U.K., on beamline 8.2. This beamline is configured with an X-ray wavelength $\lambda = 1.5$ Å. Details of the storage ring, radiation, camera geometry, and data collection electronics have been given elsewhere.[17] The sample was placed in a TA Instruments DSC pan fitted with 25 μm mica windows. The loaded pans were placed in the cell of a Linkam DSC of single-pan design. The cell comprised a silver furnace around a heat-flux plate with a 3×0.5 mm slot, the sample being held in contact with the plate by a low-thermal-mass spring. A more complete description of the DSC and the sample pans can be found elsewhere.[18] Scattered photons were collected on a multiwire quadrant positional sensitive detector located 2 m from the sample. A scattering pattern from an oriented specimen of wet collagen (rat-tail tendon) was used for calibration of the q scale range of the detector ($q = 4\pi \sin\theta/\lambda$, where the scattering angle is defined as 2θ). The experimental data were corrected for background scattering (from the camera and empty shear cell), sample absorption, and the positional alinearity of the detector.

III. Experimental Results

A. T_{ODT} from Rheology. Figure 4 shows the elastic modulus, G', for u-AB and u-A_2B_2 for increasing and decreasing temperature sweeps. From the sharp drop (rise) in G', the T_{ODT} for u-AB is determined to be between 148 and 158 °C and the T_{ODT} for u-A_2B_2 to be between 195 and 200 °C. Note that the measured value of G' for u-AB vanishes for temperatures greater than 158 °C on the heating curve and 148 °C on the cooling curve as the storage modulus falls below the sensitivity of the instrument. The hysteresis in both sets of measurements (≈10 °C for u-AB and ≈5 °C for u-A_2B_2) is due to superheating in the heating curve and supercooling in the cooling curve. Since the disordering process is much faster than the ordering process,

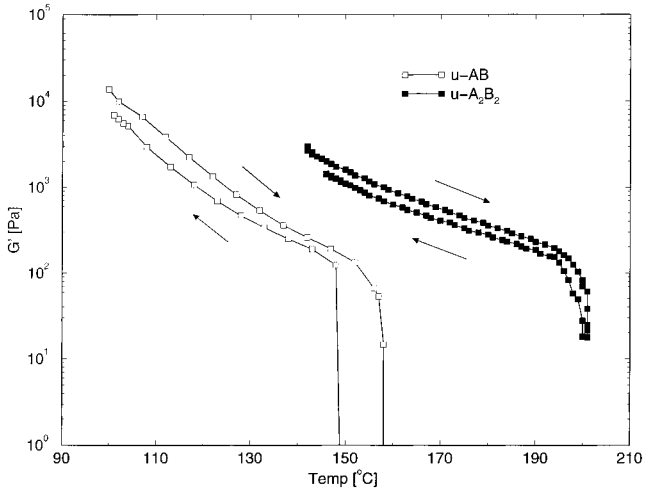

Figure 4. Elastic modulus for u-AB and u-A_2B_2 for increasing and decreasing temperature sweeps.

supercooling is more likely than superheating.[19] The heating curves therefore give a better estimate of the thermodynamic T_{ODT}, and in what follows, we shall use the value of T_{ODT} derived from the heating curve as our rheological estimate of the true T_{ODT}. Clearly, even if one accounts for the uncertainty due to hysteresis, there is a significant difference in the T_{ODT} of u-AB compared to u-A_2B_2; i.e., $\Delta T_{ODT} \approx 42$ °C. This is in contrast to the mean-field theory prediction that the T_{ODT} for these two polymers should be the same (eq 1).

One possibility for this discrepancy might be the small mismatch in the total and arm molecular weights in u-AB and u-A_2B_2 since these samples were prepared independently of each other. Calculating N using eq 27, the parameter values given in subsection IVB, and the values for M_n given in Table 1, we find $N = 252$ for u-AB and $N = 238$ for u-A_2B_2. Inserting this into eq 1 and using the temperature dependence of χ given by eq 38, we find $T_{ODT} = 288$ °C for u-AB and $T_{ODT} = 277$ °C for u-A_2B_2; i.e., $\Delta T_{ODT} \approx 11$ °C. Although this is much smaller than the observed difference, it illustrates the fact that a small mismatch in molecular weights can lead to significant differences in T_{ODT}.

A further source for a mismatch in molecular weights might be due to polydispersity. The spread in molecular weight is related to the ratio M_w/M_n by[20]

$$\frac{\langle \Delta M^2 \rangle}{M_n^2} \equiv \frac{\langle (\Delta M - M_n)^2 \rangle}{M_n^2} = \frac{M_w}{M_n} - 1$$

where M is the molecular weight, M_w and M_n are the weight- and number-averaged molecular weights, respectively, and $\langle (...) \rangle$ denotes an average over the molecular weight distribution. For our block copolymer samples which have very low polydispersity, the value of $M_w/M_n = 1.01$ measured by GPC is not very accurate because problems with instrumental broadening set a lower limit on M_w/M_n values that can be measured; the actual value of M_w/M_n is probably lower. However, assuming a value of $M_w/M_n = 1.01$ for our sample, we have a spread in molecular weights of about 10% (i.e., $\langle \Delta M^2 \rangle^{1/2}/M_n \approx 0.1$). If we further assume that the uncertainty in the measured value of M_n is of the order of $\langle \Delta M^2 \rangle^{1/2}/M_n$, this could potentially lead to a mismatch in M_n of 10% and hence a difference in T_{ODT} of 30−40 °C for our parameter values.

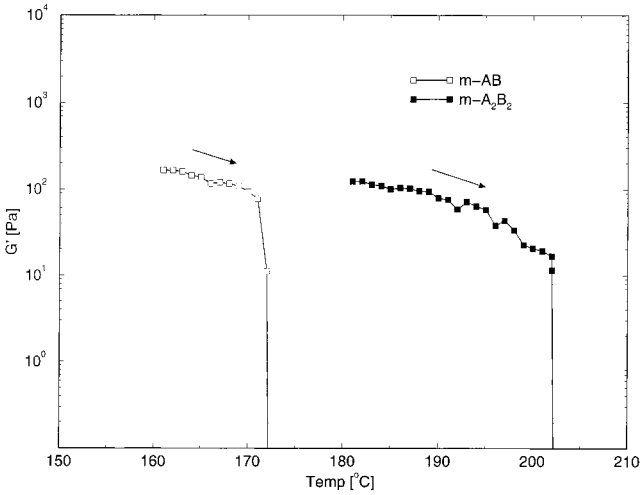

Figure 5. Elastic modulus for m-AB and m-A_2B_2 for increasing temperature sweeps.

Although the above estimation is certainly overly pessimistic, it nevertheless illustrates the fact that to perform a credible test of the mean-field theory it is vital that we minimize the mismatch in molecular weights to very low levels. To do this, AB and A_2B_2 styrene−isoprene copolymers were prepared from the same stocks of unlinked parent living polymer arms (see subsection IIA). This ensures that the resultant linear and star copolymers, denoted m-AB and m-A_2B_2, respectively, have *identical* PS and PI mean block weights. One might still be concerned that even when the mean molecular weights of the PS and PI blocks in AB and A_2B_2 are the same, the polydispersity in PS and PI block weights might influence $(\chi N)_{ODT}$ differently for different architectures, thus leading to differences in T_{ODT}. However, given the very small polydispersities in both the PS and PI blocks, this source of error can be effectively ruled out.

Figure 5 shows the elastic modulus for m-AB and m-A_2B_2 for an increasing temperature sweep (we only measured the heating curve since this gives a better estimate of T_{ODT}). We find that for m-AB $T_{ODT} \approx 172$ °C and for m-A_2B_2 $T_{ODT} \approx 202$ °C. Note that the measured value of G' for m-AB and m-A_2B_2 vanishes for temperatures greater than 172 and 202 °C, respectively, as the storage modulus falls below the sensitivity of the instrument. There is clearly a significant difference in T_{ODT} between m-AB and m-A_2B_2, $\Delta T_{ODT} \approx 30$ °C, even though it is slightly smaller than the difference between that for u-AB and u-A_2B_2. This further confirms that the observed differences in Figures 4 and 5 are not due to polydispersity effects (including a mismatch in PS, PI block molecular weights between AB and A_2B_2 and polydispersity of the PS, PI blocks). The results for T_{ODT} from this section (derived from the heating curve) are collected in Table 2.

B. T_{ODT} and q^* from SAXS. To locate T_{ODT} from SAXS, specimens were heated from 140 °C at either 2 or 4 °C min^{-1} to a temperature above the observed T_{ODT}. The ODT is apparent from a discontinuous decrease in intensity and increase in width of the first-order scattering peak.[21] In addition, the position of the first-order reflection, centered at q^*, was determined as a function of temperature. The dimensionless wave vector x^* corresponding to q^*(ODT) was also calculated from eq 37 and using parameter values given in subsection IVB. These results are collected in Table 2.

Table 2. Results for T_{ODT} and q^* from Rheology and SAXS

	T_{ODT}/°C				
sample	rheology[a]	SAXS[b]	q^*(ODT)[c]	q^*(140 °C)[c]	x^*(ODT)
u-AB	158	157	0.0368	0.0360	2.48 ± 0.05
u-A_2B_2	200	202	0.0356	0.0328	2.19 ± 0.05
m-AB	172	171	0.0364	0.0352	2.43 ± 0.05
m-A_2B_2	202	206	0.0356	0.0324	2.33 ± 0.05

[a] From heating curve of dynamic temperature sweep; estimated uncertainty, ±3 °C. [b] Estimated uncertainty, ±2 °C. [c] Estimated uncertainty, ±0.0004 Å^{-1}.

The ODT values from SAXS listed in Table 2 are in good agreement with those obtained from rheology. The difference in q^* at the ODT between AB and A_2B_2 copolymers is small but just outside the experimental uncertainty for both pairs (m and u). Further confirmation of the difference in q^* is provided by measurements at lower temperature. A reference temperature, $T = 140$ °C, was chosen because it is above $T_g(PS)$. Here q^* for the linear copolymers has barely decreased compared to the ODT, whereas q^* is much smaller for the stars compared to q^*(ODT). However, at 140 °C as well as the ODT, q^* for the AB copolymers is larger than q^* for the A_2B_2 samples. Our results for q^*, which are measured near the ODT, are consistent with the results of Turner et al.[12] far below the T_{ODT}. Turner et al. also find that q^* for AB diblocks is greater than that for A_2B_2, even after correcting for the small mismatch in molecular weights present in their samples. Finally, we note that, for all four samples, the calculated values for x^* are significantly less than $x^* = 3.785$, the value for predicted from RPA (see subsection IVA); this indicates that even at the ODT, the polymer chains are more significantly stretched compared to the RPA prediction and may in fact no longer obey Gaussian chain statistics. The differing degree of chain stretching between AB and A_2B_2 will be the key input in the simple model calculation of section V where we propose an explantion for the observed discrepancy in the T_{ODT} between linears and stars.

IV. T_{ODT} from Mean-Field Theory

A. Segmentally Symmetric Case. In this section, we outline the calculation of the spinodal of the ODT for A_nB_n heteroarm star block copolymers using Leibler's mean-field theory (or the random phase approximation).[22] Each A_nB_n polymer chain consists of n A blocks (each containing N_A monomers) joined to n B blocks (each containing N_B monomers) at a single junction point (see Figure 1). For simplicity, we shall assume that both the A and B blocks are monodisperse, which is a very good approximation for the samples in this study. We shall also assume that the A and B monomers are segmentally symmetric; i.e. both A and B have the same monomeric volume ($v_A = v_B \equiv v$) and statistical segment length ($b_A = b_B \equiv b$); the effect of segmental asymmetry will be considered in the next subsection. For the segmentally symmetric case, the volume fraction of A monomers, f, is given by

$$f = \frac{N_A}{N_A + N_B} \tag{2}$$

and $N_A = fN$, $N_B = (1 - f)N$, where $N = N_A + N_B$.

Previous authors have calculated the spinodal[5] and binodal[23] of the ODT for segmentally symmetric A_nB_n within the framework of mean-field theory. In our treatment of the spinodal, we shall employ the formalism developed by Read[24] for calculating structure factors; this results in a considerable simplification of the calculation. In general, one requires the binodal in order to calculate T_{ODT}. However, for symmetric A_nB_n ($f = 0.5$) in the segmentally symmetric case, the spinodal and binodal coincide[5] so that T_{ODT} can be calculated directly from the spinodal.

According to Leibler's mean-field theory,[22] the spinodal is given by the condition $\Gamma_2(f, q) = S(f, q)^{-1} = 0$. Here $\Gamma_2(f, q)$ is the second-order vertex function (i.e., the coefficient of the second-order term in the expansion of the system Hamiltonian in compositional variables[6,10,22]), $S(f, q)$ the static scattering structure factor, and q the scattering wave vector. It can be easily shown that $S(f, q)^{-1}$ ($\Gamma_2(f, q)$) of A_nB_n is given by the RPA to be

$$\Gamma_2(f, q) = S(f, q)^{-1} = \frac{F(f, q) - 2\chi N}{N} \tag{3}$$

where χ is the Flory interaction parameter between A and B monomers and

$$F(f, q) = \frac{s_0^{AA} + s_0^{BB} + 2s_0^{AB}}{s_0^{AA}\, s_0^{BB} - (s_0^{AB})^2} \tag{4}$$

Here s_0^{AA}, s_0^{BB}, and s_0^{AB} are the monomer−monomer correlation functions in the noninteracting limit, i.e., in the absence of excluded volume interactions and with $\chi = 0$. These are given by

$$s_0^{AA} = \frac{v\langle \rho_{\mathbf{q}}^A \rho_{-\mathbf{q}}^A \rangle_0}{N\Omega} \tag{5}$$

$$s_0^{BB} = \frac{v\langle \rho_{\mathbf{q}}^B \rho_{-\mathbf{q}}^B \rangle_0}{N\Omega} \tag{6}$$

$$s_0^{AB} = \frac{v\langle \rho_{\mathbf{q}}^A \rho_{-\mathbf{q}}^B \rangle_0}{N\Omega} \tag{7}$$

where v is the monomeric volume, Ω is the total volume of the system, and $\langle ... \rangle_0$ denotes an average over chain conformations in the absence of interactions. Also $\rho_{\mathbf{q}}^A$, $\rho_{\mathbf{q}}^B$ are the (Fourier transformed) densities of A and B respectively given by

$$\rho_{\mathbf{q}}^A = \sum_{\alpha,s} y_s^\alpha \exp(i\mathbf{q}\cdot\mathbf{r}_s^\alpha) \tag{8}$$

$$\rho_{\mathbf{q}}^B = \sum_{\alpha,s} (1 - y_s^\alpha) \exp(i\mathbf{q}\cdot\mathbf{r}_s^\alpha) \tag{9}$$

where $\mathbf{r}_s^\alpha$ is the position of the sth monomer on chain α and $y_s^\alpha = 1$ if monomer s on chain α is an A monomer and $y_s^\alpha = 0$ if it is a B monomer. Inserting eqs 8 and 9 into eqs 5−7 and noting that monomers on different chains are not correlated to each other, we can express s_0^{AA}, s_0^{BB}, and s_0^{AB} as single chain correlation functions given by

$$s_0^{AA} = \frac{1}{nN^2} \sum_{s,t} y_s y_t \langle \exp[i\mathbf{q}\cdot(\mathbf{r}_s - \mathbf{r}_t)] \rangle_0 \tag{10}$$

$$s_0^{BB} = \frac{1}{nN^2} \sum_{s,t} (1 - y_s)(1 - y_t) \langle \exp[i\mathbf{q}\cdot(\mathbf{r}_s - \mathbf{r}_t)] \rangle_0 \tag{11}$$

$$s_0^{AB} = \frac{1}{nN^2} \sum_{s,t} y_s (1 - y_t) \langle \exp[i\mathbf{q}\cdot(\mathbf{r}_s - \mathbf{r}_t)] \rangle_0 \tag{12}$$

where the summations are over monomer pairs on the same polymer chain.

The correlation functions s_0^{AA}, s_0^{BB}, and s_0^{AB} can be readily calculated using the "toolkit" of Read.[24] For details, the reader is referred to ref 24; we shall only give a brief outline here. The ingenuity of the formalism is to replace the sum over *monomers* in eqs 10−12 by a sum over *blocks* (γ), which are defined to be the individual A and B arms of A_nB_n in our case. More specifically, the correlation functions can be expressed as

$$s_0^{AA} = \frac{1}{nN^2}\left(\sum_\gamma J_\gamma^{AA} + \sum_{\gamma \neq \gamma'} H_\gamma^A H_{\gamma'}^A \right) \tag{13}$$

$$s_0^{BB} = \frac{1}{nN^2}\left(\sum_\gamma J_\gamma^{BB} + \sum_{\gamma \neq \gamma'} H_\gamma^B H_{\gamma'}^B \right) \tag{14}$$

$$s_0^{AB} = \frac{1}{nN^2}\left(\sum_{\gamma \neq \gamma'} H_\gamma^A H_{\gamma'}^A \right) \tag{15}$$

where J_γ^{AA}, J_γ^{BB} are the "self-terms" of A and B blocks, respectively, and H_γ^A, H_γ^B are the "co-terms" of A and B blocks, respectively (γ is the block index). The self-term accounts for monomer−monomer correlations within the same block, while the product of two co-terms of different blocks accounts for correlations between monomers on different blocks. For a Gaussian coil of M monomers with monomeric length b, the "self-term" is

$$J(q) = \frac{2}{{Q_0}^2} [\exp(-MQ_0^2) - 1 + MQ_0^2] \tag{16}$$

while the "co-term" is

$$H(q) = \frac{1}{{Q_0}^2} [1 - \exp(-Q_0^2 M)] \tag{17}$$

where $Q_0^2 = q^2b^2/6$. Now A_nB_n has n A blocks containing fN monomers and n B blocks containing $(1 - f)N$ monomers, all of which are assumed to be Gaussian coils. The correlation functions are therefore given by

$$s_0^{AA}(f, x) = g(f, x) + \frac{(n-1)}{x^2}(1 - e^{-fx})^2 \tag{18}$$

$$s_0^{BB}(f, x) = g(1 - f, x) + \frac{(n-1)}{x^2}(1 - e^{-(1-f)x})^2 \tag{19}$$

$$s_0^{AB}(f, x) = \frac{n}{x^2}(1 - e^{-fx})(1 - e^{-(1-f)x}) \tag{20}$$

where

$$g(f, x) = \frac{2}{x^2}[e^{-fx} - 1 + fx] \tag{21}$$

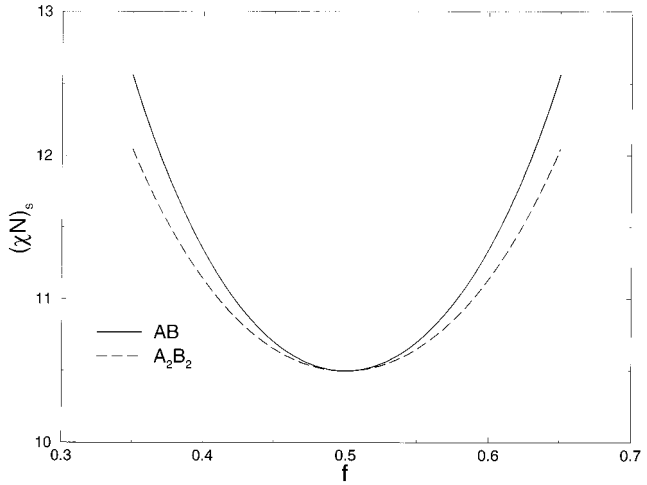

Figure 6. Mean-field theory result for the spinodal of the ODT $(\chi N)_s$ vs the volume fraction f for segmentally symmetric AB and A_2B_2.

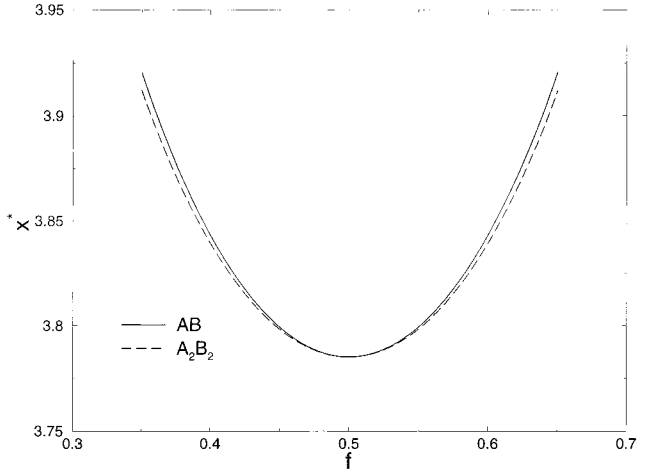

Figure 7. Mean-field theory result for the scattering peak in the disordered state x^* vs the volume fraction f for segmentally symmetric AB and A_2B_2.

is the modified Debye function, $x = NQ_0^2 = q^2R_g^2$, and $R_g^2 = Nb^2/6$ is the radius of gyration of an AB diblock.

Now $S(f, x)$ given by eq 3 has a maxima at $x = x^*$ due to a correlation hole effect and this provides the RPA prediction for the scattering peak position in the disordered phase. Also from the condition $S(f, x)^{-1} = 0$, the spinodal of the ODT is given by the RPA as

$$(\chi N)_s = F(f, x^*)/2 \tag{22}$$

In Figures 6 and 7, we plot $(\chi N)_s$ and x^* respectively as a function of f for AB and A_2B_2. We see that both the $(\chi N)_s$ and x^* at the same f are in general different for AB and A_2B_2 except at $f = {}^1/_2$ where they are the same. As explained above, the binodal $(\chi N)_{ODT}$ coincides with the spinodal $(\chi N)_s$ for $f = {}^1/_2$. We therefore have $(\chi N)_s = (\chi N)_{ODT} = 10.495$ and $x^* = 3.785$ for symmetric AB and A_2B_2. More generally, $(\chi N)_{ODT}$ and x^* are both independent of the number of arms n for symmetric A_nB_n. This surprising fact was first noted by Olvera de la Cruz and Sanchez[5] and results from the fact that the "junction constraint" imposed on A_nB_n (i.e., forming an A_nB_n from n AB diblocks) lowers the entropy of both the disordered and ordered phase at ODT by the same amount for $f = {}^1/_2$. We can also understand this fact mathematically using eqs 18−20. For $f = {}^1/_2$, we have

$$s_0^{AA}({}^1/_2, x) = s_0^{BB}({}^1/_2, x)$$
$$= g({}^1/_2, x) + \frac{(n-1)}{x^2}(1 - e^{-x/2})^2 \tag{23}$$

$$s_0^{AB}({}^1/_2, x) = \frac{n}{x^2}(1 - e^{-x/2})^2 \tag{24}$$

so that

$$F({}^1/_2, x) = \frac{2}{s_0^{AA}({}^1/_2, x) - s_0^{AB}({}^1/_2, x)}$$
$$= \frac{2}{g({}^1/_2, x) - \frac{1}{x^2}(1 - e^{-x/2})^2} \tag{25}$$

which is independent of n. Hence $(\chi N)_{ODT}$ and x^* are also independent of n. Clearly the RPA, assuming segmentally symmetric A and B monomers, fails to predict the significant difference in T_{ODT} found experimentally. In the next subsection we include the effect of segmental asymmetry to see if this can explain the experimental result.

B. Effect of Segmental Asymmetry. In this subsection, we calculate $(\chi N)_s$ for an A_nB_n block copolymer including segmental asymmetry. As before, each A_nB_n consists of n A blocks containing N_A monomers and n B blocks containing N_B monomers all joined at a single point, but now $v_A \neq v_B$ and $b_A \neq b_B$. In this case, care needs to be taken in how one defines f, N_A, N_B, and N. We shall adopt the usual experimental definition as follows. We define f and N as

$$f = \frac{\frac{M_{n,A}}{\rho_A}}{\frac{M_{n,A}}{\rho_A} + \frac{M_{n,B}}{\rho_B}} \tag{26}$$

$$N = \frac{\frac{M_{n,A}}{\rho_A} + \frac{M_{n,B}}{\rho_B}}{\left(\frac{M_A}{\rho_A}\frac{M_B}{\rho_B}\right)^{1/2}} \tag{27}$$

where $M_{n,A}$, $M_{n,B}$ are the number-averaged molecular weights of the A and B blocks respectively, M_A, M_B are the molecular weights of the A and B monomers, respectively, and ρ_A, ρ_B are the mass densities of A and B respectively. The quantities N_A, N_B are then defined as

$$N_A = fN \qquad N_B = (1 - f)N \tag{28}$$

The segmental asymmetry introduces an extra parameter controlling phase behavior known as the segmental asymmetry parameter. In the weak segregation limit, this is given by[25,26]

$$\epsilon \equiv \frac{R_{gA}{}^2/V_A}{R_{gB}{}^2/V_B} = \frac{b_A{}^2/v_A}{b_B{}^2/v_B} \tag{29}$$

where $R_{gA} = (N_A b_A{}^2/6)^{1/2}$, $R_{gB} = (N_B b_B{}^2/6)^{1/2}$ is the radius of gyration of an A and B block, respectively, and $V_A =$

$N_A v_A$, $V_B = N_B v_B$ is the volume occupied by an A and B block, respectively. (Note that this is different from the strong segregation case where the number of A and B blocks in the heteroarm star polymer, i.e., n_A, n_B, respectively, also enters into the expression for the asymmetry parameter. The asymmetry parameter in this case, ϵ_{SSL}, is given by[27] $\epsilon_{SSL} = (n_B/n_A)^2(R_{gA}^2/V_A)/(R_{gB}^2/V_B)$.) Going through the same calculation of the scattering structure factor as before, it is easy to show that eq 3 is modified to

$$\Gamma_2(f, x, \epsilon) = S(f, x, \epsilon)^{-1} = \frac{F(f, x, \epsilon) - 2\chi N}{N} \quad (30)$$

where

$$F(f, x, \epsilon) = \frac{s_0^{AA}(f, x, \epsilon) + s_0^{BB}(f, x, \epsilon) + 2s_0^{AB}(f, x, \epsilon)}{s_0^{AA}(f, x, \epsilon)s_0^{BB}(f, x, \epsilon) - (s_0^{AB}(f, x, \epsilon))^2} \quad (31)$$

Here, s_0^{AA}, s_0^{BB}, and s_0^{AB} are the modified correlation functions given by

$$s_0^{AA}(f, x, \epsilon) = g(f, x_A) + \frac{(n-1)}{x_A^2}(1 - e^{-fx_A})^2 \quad (32)$$

$$s_0^{BB}(f, x, \epsilon) = g(1-f, x_B) + \frac{(n-1)}{x_B^2}(1 - e^{-(1-f)x_B})^2 \quad (33)$$

$$s_0^{AB}(f, x, \epsilon) = \frac{n}{x_A x_B}(1 - e^{-fx_A})(1 - e^{-(1-f)x_B}) \quad (34)$$

where

$$x_A = \frac{x}{f + (1-f)/\epsilon} \quad (35)$$

$$x_B = \frac{x}{f\epsilon + (1-f)} \quad (36)$$

with

$$x = \frac{q^2}{6}(N_A b_A^2 + N_B b_B^2) \quad (37)$$

We shall use the following parameter values from the literature and Table 1: $\rho_S = 0.969$ g/cm^3; $\rho_I = 0.83$ g/cm^3; $b_S = 6.7$ Å; $b_I = 6.5$ Å;[28] $M_{n,S} = 11\,500$ g mol^{-1}; $M_{n,I} = 9840$ g mol^{-1} (i.e. for the m samples); $M_S = 104$ g mol^{-1}; $M_I = 68$ g mol^{-1}. Inserting these values into eqs 26, 27, and 29, we get $f = 0.50$, $N = 253$, and $\epsilon = 1.2$ (we have defined I = A and S = B so that $\epsilon > 1$). In Figure 8, we plot $(\chi N)_s$ as a function of f for AB and A_2B_2 for $\epsilon = 1.2$. The effect of $\epsilon > 1$ is to shift the spinodal curves of both AB and A_2B_2 to the right but by different amounts. This results in a small difference in $(\chi N)_s$ between AB and A_2B_2 at $f = 0.5$: $(\chi N)_s = 10.504$ for AB and $(\chi N)_s = 10.497$ for A_2B_2. Using the temperature-dependence of the χ parameter reported by Mori et al.[29]

$$\chi(T) = \frac{66}{T} - 0.0937 \quad (38)$$

the spinodal temperature of m-AB and m-A_2B_2 are given by $T_s = 215.0$ °C and $T_s = 215.1$ °C, respectively; i.e., $\Delta T_s \approx 0.1$ °C. Note that the coincidence of the binodal and spinodal at $f = 0.5$ is no longer strictly true for $\epsilon \neq 1$. However since the degree of segmental asymmetry is small in our case (i.e., ϵ close to unity), we expect the spinodal to be very close to the binodal; we shall therefore equate the binodal with the spinodal. The effect of segmental asymmetry is therefore negligible and cannot explain the experimental difference in T_{ODT}.

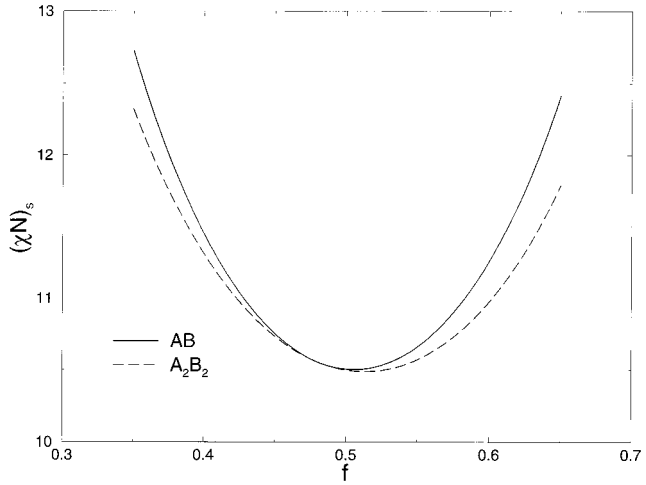

Figure 8. Mean-field theory result for the spinodal of the ODT $(\chi N)_s$ vs the volume fraction f for AB and A_2B_2 with segmental asymmetry $\epsilon = 1.2$.

V. Effect of Compositional Fluctuations

A. Brazovskii−Fredrickson−Helfand Calculation. In the RPA, local compositional fluctuations about the mean compositional profile are neglected. These fluctuations, however, become important near the ODT for symmetric block copolymers, and they lower T_{ODT} (i.e., raise $(\chi N)_{ODT}$).[6] A possible explanation for the observed difference in T_{ODT} therefore might be different strengths of compositional fluctuations due to differences in molecular architecture. Using a self-consistent one loop calculation first developed by Brazovskii,[30] Fredrikson and Helfand[6] calculated the shift in T_{ODT} due to compositional fluctuations in diblock copolymer. In order to obtain analytically tractable results, they made the simplifying assumption that the third- and fourth-order vertex functions, Γ_3 and Γ_4, respectively, have no wave vector dependence. A consequence of this assumption is that the scattering peak position remains at the mean-field value of $x^* = x^*_{MF} = 3.785$, independent of N, i.e., $q^* \sim R_g^{-1} \sim N^{-1/2}$. This means that the block copolymer chains are effectively assumed to be Gaussian, as in the RPA. In what follows, we refer to this theory as the Fredrickson−Helfand (FH) theory. For symmetric block copolymers ($f = 1/2$) FH theory gives

$$(\chi N)_{ODT} = (\chi N)_s + 1.0154c^2(d\lambda)^{2/3}\bar{N}^{-1/3} \quad (39)$$

where

$$c = \left[\frac{1}{3}x\frac{\partial^2 F(f, x)}{\partial x^2}\right]^{1/2}_{x=x^*}$$

$$d = 3x^*/2\pi$$

$$\lambda = N\Gamma_4(0, 0)/c^4$$

$$\bar{N} = \frac{b^6}{v^2}N$$

Here $(\chi N)_s$, x^* are the RPA values of the spinodal and scattering peak position, respectively, $\Gamma_4(0, 0)$ is the fourth-order vertex function defined in refs 6 and 22 with its arguments set to zero, and $v^2 = v_A v_B$, $b^2 = f b_A^2 + (1 - f) b_B^2$. Note that we have relaxed the original constraint imposed in ref 6 of $v = b^3$, so that the fluctuation correction is controlled by $\bar{N}$ and not N (see refs 10 and 26).

The quantities $(\chi N)_s$, c, and d are readily calculated from the results in subsection IVA; they are the same for both AB and A_2B_2 (since $F(^1/_2, x)$ is the same, see eq 25); i.e., $(\chi N)_s = 10.495$, $c = 1.1019$, and $d = 1.807$. The expression for Γ_4 for AB diblocks is explicitly given in refs 22 and 31. From these results, we find $\lambda = 106$ for symmetric AB ($f = 0.5$). Dobrynin and Erukhimovich[23,32] have calculated Γ_4 for the general case of A_nB_n, but unfortunately they do not give the expression explicitly. However, they give explicit results for $\alpha = (\chi N)_{ODT}^{fluc}/(\chi N)_{ODT}^{MFT}$ evaluated at specific values of N for both AB and A_2B_2 (Figure 6b of ref 32), where $(\chi N)_{ODT}^{fluc}$ and $(\chi N)_{ODT}^{MFT}$ are the fluctuation corrected and mean-field values respectively of the binodal of the ODT.[33] The calculation of Dobrynin and Erukhimovich is also based on Brazovskii's self-consistent one loop calculation, but in contrast to Fredrickson−Helfand, they retain the wave vector dependence of Γ_4 in their calculation. The scattering peak position is however fixed at the mean-field value of $x^* = x^*_{MF} = 3.785$. Despite the difference in the Dobrynin−Erukhimovich and FH approaches, the values of $(\chi N)_{ODT}$ (or α) calculated from both approaches are practically the same: for AB with $f = 0.5$, $N = 10^4$, Dobrynin−Erukhimovich give $(\chi N)_{ODT} = 12.46 \pm 0.03$, $\alpha = 1.187 \pm 0.003$, while FH give $(\chi N)_{ODT} = 12.40$, $\alpha = 1.181$ (using eq 39 and assuming $v = b^3$ as in ref 32, so that $\bar{N} = N$); for AB with $f = 0.5$, $N = 10^6$, Dobrynin−Erukhimovich give $(\chi N)_{ODT} = 10.94 \pm 0.03$, $\alpha = 1.042 \pm 0.003$, while FH give $(\chi N)_{ODT} = 10.90$, $\alpha = 1.039$. Given the small discrepancy in $(\chi N)_{ODT}$ between the two approaches (less than 0.5%), we can obtain a very good estimate of λ for A_2B_2 using the results of Dobrynin−Erukhimovich and eq 39.

For AB with $f = 0.5$, $\alpha = 1.187 \pm 0.003$ for $N = 10^4$ and $\alpha = 1.042 \pm 0.003$ for $N = 10^6$, which gives $\lambda = 111 \pm 3$ and $\lambda = 118 \pm 13$, respectively. The estimated values for λ are in good agreement with each other and with the exact value of $\lambda = 106$ (especially the value derived from $N = 10^4$, which is more accurate). For A_2B_2 with $f = 0.5$, $\alpha = 1.147 \pm 0.003$ for $N = 10^4$ and $\alpha = 1.033 \pm 0.003$ for $N = 10^6$, which give $\lambda = 78 \pm 2$ and $\lambda = 82 \pm 11$, respectively, in good agreement with each other. In what follows, we shall use $\lambda = 80$ for A_2B_2. On the basis of our estimation of λ for AB, we expect the error in the value of λ for A_2B_2 to be less than 5%. The resultant calculation of the fluctuation correction to $(\chi N)_{ODT}$ (within the framework of FH theory) should therefore be accurate to within 3%.

From the parameter values given in subsection IVB we find $\bar{N} = 860$ for m-AB and m-A_2B_2. Inserting this and the parameter values given above into eq 39, we have $(\chi N)_{ODT} = 14.8$ for m-AB and $(\chi N)_{ODT} = 14.1$ for m-A_2B_2. Using $\chi(T)$ given by eq 38, this gives $T_{ODT} = 161$ °C for u-AB and $T_{ODT} = 169$ °C for u-A_2B_2; i.e., $\Delta T_{ODT} = 8$ °C. While the difference is significant, it is too small to explain the experimentally observed difference of $\Delta T_{ODT} \approx 30$ °C. In the next subsection, we incorporate the effect of non-Gaussian stretching (neglected in the FH and Dobrynin−Erukhimovich treatments) into a fluctuation calculation to see what effect this has on T_{ODT}.

B. Effect of Non-Gaussian Chain Stretching on T_{ODT}. In the calculation of Fredrickson and Helfand, the block copolymer chains were assumed to adopt Gaussian chain conformations. However from analytical theory[9,10] as well as computer simulations,[8] it has been found that because of the clustering of like monomers near the ODT, the polymer chains are actually stretched in order to minimize the overlap between the A and B blocks and lower the total energy of the system; i.e., the A and B blocks are "polarized". In contrast, the clustering of like monomers appears to only weakly influence the conformational statistics of the individual A and B blocks. The resultant conformation of block copolymer chains near the ODT therefore resembles a "dumbell" shape rather than a random Gaussian coil. As a result of chain polarization, the scaling of $q^* \sim N^{-\delta}$ changes from $\delta = 0.5$ (Gaussian) to $\delta \approx 0.8$. This deviation from Gaussian behavior, induced by dissimilar segmental interactions, has been well established from previous experimental studies[7] and is what we have termed "non-Gaussian stretching" in this paper. The non-Gaussian stretching of block copolymer chains is very effective at reducing q^* (the principal scattering peak) below the RPA value of $x^* = 3.785$, especially for temperatures near T_{ODT} (see ref 7). Given that we are working at or near the ODT, we conclude that non-Gaussian stretching is the underlying reason why $x^* < 3.785$ in all our samples (see Table 2). Non-Gaussian stretching also has a significant effect on the ODT; it increases the tendency of the block copolymer to microphase separate, thereby decreasing $(\chi N)_{ODT}$ (increasing T_{ODT}).[10,13] Given that, experimentally, the A_2B_2 chains appear to be more strongly stretched compared to their AB analogs (i.e., $x^*(A_2B_2) < x^*(AB)$; see Table 2), we expect this effect to lead to A_2B_2 having a higher T_{ODT} compared to AB. Incorporating non-Gaussian stretching into a fluctuation theory could therefore lead to the observed differences in T_{ODT}.

In order to obtain a rigorous fluctuation theory which correctly incorporates non-Gaussian stretching, one should evaluate the full partition sum of the block copolymer system, taking care not to quench the chain stretching degree of freedom. Such a calculation was performed by Olvera de la Cruz[9] and Barrat and Fredrickson[10] for AB diblocks within the framework of the self-consistent one-loop approximation. However, in contrast to the earlier calculations by Fredrickson−Helfand and Dobrynin−Erukhimovich, these authors relaxed the constraint $x^* = x^*_{MF} = 3.785$ in their calculation. This allowed the shift in q^* (i.e., chain stretching) and the resultant shift in T_{ODT} to be calculated. (We note that there are slight differences in the approaches of Olvera de la Cruz and Barrat−Fredrickson: denoting the full wave vector dependence of Γ_4 as Γ_4 ($\mathbf{q}$, $-\mathbf{q}$, $\mathbf{k}$, $-\mathbf{k}$), Olvera de la Cruz retains the dependence of Γ_4 on the magnitude of $\mathbf{q}$ but neglects its dependence on the angle between $\mathbf{q}$ and $\mathbf{k}$ while Barrat−Fredrickson retain the full wave vector dependence of Γ_4. However, given that the angular dependence of Γ_4 is weak,[10,34] the two approaches give nearly identical results.[34]) The extension of this calculation to the case of A_2B_2 is nontrivial as it requires knowledge of the wave vector dependence of Γ_4 and is therefore beyond the scope of this paper. In addition, while providing valuable insight into the phenomenon of non-Gaussian stretching, both the Olvera de la Cruz and Barrat−Fredrickson ap-

proaches have the drawback that they appear to underpredict the shift in T_{ODT} and q^* due to non-Gaussian stretching.[13]

In this paper, we shall instead use a simplified approach due to Maurer et al.,[13] which gives us a simple recipe for estimating the change in the mean-field value of the spinodal, $(\chi N)_s$, given the measured degree of chain stretching (i.e., q^*). The basic idea behind the approach is to model the chain polarization by constraining the center of mass of the A and B blocks to be separated by a fixed distance; this distance is chosen so that the resultant q^* from the model agrees with the experimentally measured value. Once $(\chi N)_s$ (modified for chain stretching) has been determined, $(\chi N)_{ODT}$ is then calculated by augmenting $(\chi N)_s$ with the contribution from compositional fluctuations using FH theory, i.e. eq 39. Our key objective is to see if, by incorporating sufficient chain stretching for both AB and A_2B_2 to match their respective experimental values of q^*, we also simultaneously obtain differences in T_{ODT} which are comparable to those observed experimentally. It should be emphasized that although the model we have outlined above is conceptually appealing, it is not very rigorous and involves some uncontrolled approximations. Specifically, both the way that chain polarization is modeled and the way that $(\chi N)_{ODT}$ is calculated by combining the chain stretched results and FH theory are rather ad hoc. Despite these drawbacks, there is indirect evidence, based on attempts to harmonize $\chi(T)$ measured from diblock copolymer melts and homopolymer blends, showing that the approach gives reasonable estimates for the shift in T_{ODT} due to chain stretching.[13] The model has the further advantage of being very robust, as it is insensitive to the actual microscopic mechanism causing the chain stretching. This means that although the most likely cause of the molecular stretch is due to dissimilar monomer interactions between clusters of like monomers as explained earlier, other mechanisms, e.g., the stiffening of polymer chains as the temperature is lowered, nonideal chain behavior near the branch point of A_2B_2 due to crowding effects, etc., are not precluded by the model. Bearing in mind the limitations of the theory, we shall therefore apply this model to our problem.

First of all, we calculate the shift in the mean-field value of $(\chi N)_s$ due to non-Gaussian stretching. For simplicity, we shall assume that the A and B monomers are segmentally symmetric and restrict consideration to symmetric block copolymers, $f = {}^1/_2$. The original model of Maurer et al. was applied to AB diblocks. The generalization to A_nB_n is straightforward. Given that the clustering of like monomers only has a weak effect on the conformational statistics of the individual A and B blocks, we model the A−A and B−B monomer correlation functions using the unconstrained Gaussian chain averages given by eqs 18 and 19. For symmetric A_nB_n ($f = {}^1/_2$), this gives

$$s_0^{AA}(x) = s_0^{BB}(x) = g({}^1/_2, x) + \frac{(n-1)}{x^2}(1 - \exp[-x/2])^2 \tag{40}$$

The effect of chain polarization is modeled by constraining the center of mass of the A and B blocks to be separated by a fixed distance d when computing the Gaussian chain average. The A−B correlation function is therefore given by the constrained Gaussian chain average

$$s_c^{AB} = \frac{1}{nN^2}\sum_{s,t} y_s\,(1 - y_t)\langle \exp[i\mathbf{q}(\mathbf{r}_s - \mathbf{r}_t)]\rangle_c \tag{41}$$

where s, t are monomer indices defined in Figure 1. Equation 41 is the same as eq 12 except for the fact that the nonconstrained average $\langle ... \rangle_0$ has been replaced by the constrained average $\langle ... \rangle_c$. The constrained average is defined as

$$\langle (...) \rangle_c \equiv \frac{\int d\mathbf{u} \langle (...)\delta[\mathbf{u}d - (\mathbf{X}_A - \mathbf{X}_B)]\rangle_0}{\int d\mathbf{u} \langle \delta[\mathbf{u}d - (\mathbf{X}_A - \mathbf{X}_B)]\rangle_0} \tag{42}$$

where $\mathbf{u}$ is a unit vector that is integrated over the unit sphere and $\delta[\mathbf{r}]$ is the three-dimensional Dirac delta function. The constrained average above is the same as the one used in Maurer et al. for AB diblocks, but $\mathbf{X}_A$, $\mathbf{X}_B$ are now the *collective* centers of mass of the A and B blocks, respectively, given by

$$\mathbf{X}_A = \frac{2}{nN}\left\{\sum_{p=1}^{n} \int_{(p-1)N}^{(p-1/2)N} \mathbf{r}(s)\, ds\right\}$$

$$\mathbf{X}_B = \frac{2}{nN}\left\{\sum_{p=1}^{n} \int_{(p-1/2)N}^{pN} \mathbf{r}(s)\, ds\right\} \tag{43}$$

The way that we have modeled A and B polarization in A_nB_n contains important physics. Due to chain connectivity, the response of the n A blocks to dissimilar segmental interactions are highly correlated to each other and likewise for the n B blocks. Therefore, instead of considering the individual response of the A (or B) blocks, we can group the n A (or B) blocks together as a single entity and considered consider their collective response to dissimilar segmental interactions. Note that the unconstrained root-mean-square average separation between the A and B centers of mass for A_nB_n is given by

$$\langle (\boldsymbol{X}_A - \boldsymbol{X}_B)^2 \rangle_0^{1/2} = \sqrt{\frac{2}{n}}\, R_g \tag{44}$$

By symmetry, we have

$$\sum_{s,t} y_s\,(1 - y_t)\,\langle \exp[i\mathbf{q}(\mathbf{r}_s - \mathbf{r}_t)]\rangle_c = n^2 \int_0^{N/2} ds \int_{N/2}^{N} dt \langle \exp[i\mathbf{q}(\mathbf{r}(s) - \mathbf{r}(t))]\rangle_c \tag{45}$$

so that

$$s_c^{AB}(x, D) = \frac{n}{N^2}\int_0^{N/2} ds \int_{N/2}^{N} dt \langle \exp[i\mathbf{q}(\mathbf{r}(s) - \mathbf{r}(t))]\rangle_c \tag{46}$$

The quenched average in eq 46 can be handled analytically by inserting the the parametrization of the delta function given by $\delta[\mathbf{r}] = \int d\mathbf{y} \exp(i\mathbf{y}\cdot\mathbf{r})$ into eq 41. Performing the unconstrained Gaussian conformational averages, the required integrals over $\mathbf{y}$ and angular integrals over $\mathbf{u}$, and introducing some convenient rescalings, we find

$$s_c^{AB}(x, D) = n \int_0^{1/2} ds \int_{1/2}^{1} dt\, e^{-x(t+s-1/2)} e^{12xh(s,t)^2/n} \times \frac{\sin[6h(s, t)\sqrt{2xD^2/n}]}{6h(s, t)\sqrt{2xD^2/n}} \quad (47)$$

In this expression, D is the dimensionless distance of separation between the A and B centers of mass

$$D \equiv \frac{d}{\langle(\mathbf{X}_A - \mathbf{X}_B)^2\rangle_0^{1/2}} = \sqrt{\frac{n}{2}}\frac{d}{R_g} \quad (48)$$

and

$$h(s, t) = {}^1/_2[s(1 - s) + ({}^3/_2 - t)(t - {}^1/_2)] \quad (49)$$

Note that because we have completely integrated out **y**, our expression for $s_c^{AB}(x, D)$ is more compact compared to that of Maurer et al.,[13] involving only two numerical quadratures instead of three. This means that a full numerical evaluation of $s_c^{AB}(x, D)$ is much more tractable using eq 47. It is also more general, being applicable to all A_nB_n block copolymers; setting $n = 1$, we recover the special case of AB diblocks. However, in order to obtain an analytical expression for $s_c^{AB}(x, D)$ which is easier to handle numerically, we expand the sin factor and the $\exp[12xh(s, t)^2/n]$ factor about the origin (assuming the respective arguments to be small). Carrying out the expansion to second order in $h(s, t)$, we find

$$s_c^{AB}(x, D) \approx s_0^{AB}(x) - {}^3/_8(D^2 - 1)M(x) \quad (50)$$

where $s_0^{AB}(x)$ is the unconstrained A−B correlation function given by eq 20 (with $f = {}^1/_2$), and

$$M(x) = x^{-5}\{448[1 - \exp(-x/2)]^2 - 256x[1 - \exp(-x/2)] + 16x^2[3 - 2\exp(-x)] - 8x^3\exp(-x/2) - x^4[\exp(-x/2) - 2\exp(-x)]\} \quad (51)$$

The function $M(x)$ vanishes in the limits $x \to 0$ and $x \to \infty$ and exhibits a single maximum at $x = 1.8184$. Rather surprisingly, eq 50 is the same as the expression for $s_c^{AB}(x, D)$ given by Maurer et al. for AB diblocks (eq A9 in ref 13); the only way that n enters into the above expression is via the unconstrained A−B correlation function $s_0^{AB}(x)$ and the dimensionless distance D. The model predictions for x^* and $(\chi N)_s$ can be calculated using the function

$$F(x, D) = \frac{s_0^{AA}(x) + s_0^{BB}(x) + 2s_c^{AB}(x, D)}{s_0^{AA}(x)\, s_0^{BB}(x) - [s_c^{AB}(x, D)]^2} \quad (52)$$

with s_0^{AA}, s_0^{BB} given by eq 40 and $s_c^{AB}(x, D)$ given by eq 50. This simplifies to

$$F(x, D) = \frac{2}{s_0^{AA}(x) - s_c^{AB}(x, D)} \quad (53)$$

in our case since $s_0^{AA} = s_0^{BB}$. Equation 52 is a modified version of the $F(x)$ function in Leibler's theory given by eq 4. The value of x that minimizes $F(x, D)$ (for a given D) gives us x^* while the location of the spinodal is given by

$$(\chi N)_s = F(x^*, D)/2 \quad (54)$$

It should be pointed out here that even for $D \sim 1$, the small $h(s, t)$ expansion that has been used to derive eq 50 is strictly speaking not very accurate since $h(s, t) \sim 1$ for some values of $0 \le s \le {}^1/_2$ and ${}^1/_2 \le t \le 1$. The resultant expression however captures the proper asymptotic behavior of eq 47 for both $x \to 0$ and $x \to \infty$, and we have checked that it gives results for $F(x, D)$ which are accurate to better than 20% for all $x \ge 0$. It has the further advantage that, for $D = 1$ (i.e., the constrained distance between block centers of mass d is equal to the unconstrained root-mean-square average distance), we recover the unconstrained A−B correlation function $s_0^{AB}(x)$. This ensures that, for the unstretched "ground state" (i.e., $D = 1$), we recover the mean-field result that $(\chi N)_s$ is the same for all A_nB_n, independent of n (a property not possessed by the exact expression given by eq 47). For these reasons, we have used eq 50 for $s_c^{AB}(x, D)$ in our calculation.

As stated at the beginning of this section, our key objective is to see whether incorporating sufficient chain stretching (D) into both AB and A_2B_2 to match their respective experimental values of q^* simultaneously yields differences in T_{ODT} which are of the same order of magnitude as what is found experimentally. To achieve this objective, for a given experimental x^*, we need to find the corresponding value of D that causes $F(x, D)$ (eq 53) to be minimized at that given x^*. This defines a function $D(x^*)$ which is readily obtained by solving the quadratic equation (in D) given by $\partial F(x, D)/\partial x^* = 0$ for D given x^*. The resultant expression for $D(x^*)$ is however lengthy and is therefore not reproduced here. Once $D(x^*)$ has been obtained, the value of $(\chi N)_s$ corresponding to x^* can be evaluated from eq 54.

Finally, to calculate $(\chi N)_{ODT}$, we insert the expression for $(\chi N)_s$ given by eq 54 into eq 39. We shall assume that the fluctuation correction to $(\chi N)_{ODT}$ (i.e., the second term on the right-hand side of eq 39) is decoupled from non-Gaussian chain stretching. This allows us to use the unstretched chain results for c, d, and λ in eq 39; i.e., $c = 1.1019$, $d = 1.807$, $\lambda = 106$, 80 for AB and A_2B_2 respectively.

Figures 9 and 10 show D and $(\chi N)_s$ respectively as a function of x^* for A_nB_n. Surprisingly, both the curves are independent of n. This is because upon inserting eq 50 into eq 53, the resultant expression for $F(x, D)$ is independent of n (except implicitly in D). In Figure 9, we see that D increases for decreasing x^*; i.e., increasing chain stretching decreases x^* as expected. For $x^* = 3.785$, we recover $D = 1$. However, at $x^* = 1.8184$, there is a divergence in D. This represents a break down in the approximate expression for s_c^{AB} given by eq 50. Using this expression in $F(x, D)$, for $D \to \infty$, $F(x, D) \to (D^2M(x))^{-1}$, so that, regardless of how big D is, x^* (the minima of $F(x, D)$) can never be reduced below $x^* = 1.8184$, i.e., the position of the maxima for $M(x)$. In reality of course, for large values of D, the approximation $\sin x/x \approx 1 - x^2/6$ that was used to derive eq 50 breaks down, as higher order terms become important. These terms will cause x^* to continue to decrease below $x^* = 1.8184$ as we increase D. For large values of D, therefore, we need the full integral expression given by eq 47 to evaluate s_c^{AB}. The approximate expression given by eq 50 is only valid for $D \sim 1$ or $x^* > 2$ (see Figure 9).

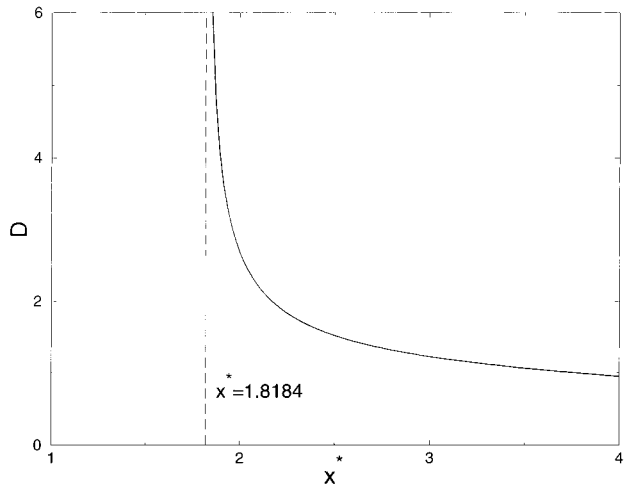

Figure 9. Dimensionless distance of separation between the A and B block centers of mass D vs the scattering peak position x^* for A_nB_n from the model of Maurer et al.

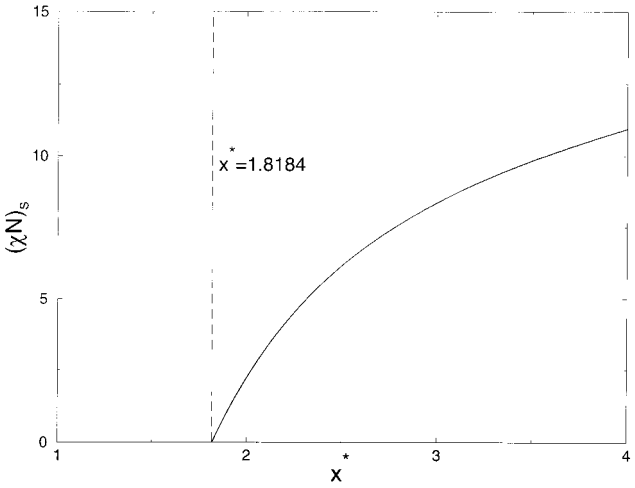

Figure 10. Spinodal of the ODT $(\chi N)_s$ vs the scattering peak position x^* for A_nB_n from the model of Maurer et al.

In Figure 10, we see that $(\chi N)_s$ decreases as we decrease x^*; i.e., increasing the degree of chain polarization increases the tendency of both block copolymers to microphase separate. For $x^* = 3.785$, we recover the Leibler mean field prediction of $(\chi N)_s = 10.5$. The value of $(\chi N)_s$ vanishes at $x^* = 1.8184$. This is again an unphysical result due to the breaking down of the approximate expression used for s_c^{AB}: for $D \to \infty$, $(\chi N)_s \to (D^2 M(x^*))^{-1} \to 0$. As in Figure 9, the curve given in Figure 10 is only physically realistic for $x^* > 2$. Given that the function $(\chi N)_s(x^*)$ is identical for all A_nB_n (Figure 10) and that experimentally we find AB has a higher value of $(\chi N)_s$ compared to A_2B_2, for our model to be self-consistent, we require the value of x^* for AB to be greater than A_2B_2 at ODT. This is indeed what we find experimentally for both pairs of samples, u and m (see Table 2).

In Table 3, we list the SAXS values of x^* for both the m and u samples together with the corresponding values of D, $(\chi N)_s$, $(\chi N)_{ODT}$, and T_{ODT}. The value of T_{ODT} has been calculated from $(\chi N)_{ODT}$ using $\chi(T)$ given by eq 38 and N given by eq 27. The uncertainty in T_{ODT} has been estimated from the experimental uncertainty in x^*; the rather large uncertainties in T_{ODT} compared to ΔT_{ODT} are due to differences in q^* which are close to the instrumental resolution limit. For all the samples, we see that D is significantly greater than unity, indicating the presence of strong chain stretching in all the samples. We also note that the small differences in the measured values of x^* (q^*) are sufficient to give rise to significant differences in $(\chi N)_{ODT}$ and T_{ODT}, comparable to what is measured experimentally. For u-AB and u-A_2B_2, the calculated difference is $\Delta T_{ODT} = 34 \pm 8$ °C while the measured difference (from Table 2) is $\Delta T_{ODT} = 44 \pm 3$ °C. For m-AB and m-A_2B_2, the calculated difference is $\Delta T_{ODT} = 21 \pm 6$ °C while the measured difference is $\Delta T_{ODT} = 32 \pm 3$ °C. We note that the theoretical model only underpredicts ΔT_{ODT} by about 30%. Given the ad hoc nature of the theoretical model, the agreement between theory and experiment is surprisingly good.

Table 3. Predictions of Simple Model Calculation for Chain Stretching and T_{ODT}

sample	x^*	D	$(\chi N)_s$	$(\chi N)_{ODT}$	T_{ODT}/°C
u-AB	2.48 ± 0.05	1.54	6.03	10.3	217 ± 4
u-A_2B_2	2.19 ± 0.05	1.95	4.04	7.7	251 ± 7
m-AB	2.43 ± 0.05	1.59	5.74	10.0	222 ± 4
m-A_2B_2	2.33 ± 0.05	1.71	5.09	8.7	243 ± 5

As the model requires the experimental value of x^*(ODT) as an input parameter, one important issue not addressed by the model is why A_2B_2 is more strongly stretched compared to AB. To obtain a proper answer to this question, one would have to at least perform a self-consistent one loop calculation similar to that of Olvera de la Cruz[9] or Barrat and Fredrickson[10] (where q^* is left as a free parameter that can be optimized), which is beyond the scope of this paper. We propose to do this in a future publication. Here, we offer the following qualitative explanation for the effect. If we imagine tying two AB diblocks together at their junction points to form an A_2B_2 molecule, the resultant junction constraint increases the A−B correlations near the branch point. This enhances the strength of dissimilar segment interactions near the branch points which induces the A and B blocks to separate. Hence, if stretching effects are important near the ODT (as indeed they are, according to experiments), we expect A_2B_2 to stretch more easily compared to AB and, hence, to microphase separate at a higher temperature.

VI. Conclusions

Symmetric styrene−isoprene diblock copolymer AB and its hetero-four-arm star analog A_2B_2 were synthesized using anionic polymerization. For the m-AB and m-A_2B_2 samples, care was taken to ensure that the arm molecular weights for both AB and A_2B_2 were matched. Measuring the T_{ODT} of both u and m samples using dynamic mechanical spectroscopy and small-angle X-ray scattering, a significant difference in T_{ODT} was found between AB and A_2B_2, contrary to mean-field theory predictions. We showed that the difference is too large to be accounted for by polydispersity, segmental asymmetry, or a Fredrickson−Helfand (FH) calculation of the fluctuation correction to the mean-field theory. We instead suggest that the effect arises from a combination of compositional fluctuations *and* differing degrees of non-Gaussian stretching in the two systems at ODT. The stretching of the polymer chains is most likely due to dissimilar interactions between clusters of like monomers, though other mechanisms (e.g., chain stiffening, crowding effects near star branch point, etc.) are not precluded. The presence of chain stretching at ODT is confirmed by SAXS measurements; for both u and m

samples, q^* is found to be less than that of a Gaussian chain of equivalent molecular weight (i.e. $x^* < 3.785$). Also at ODT, A_2B_2 stars are found to be more strongly stretched compared to their linear AB counterparts so that $x^*(AB) > x^*(A_2B_2)$. The difference in x^* (q^*) is accentuated when measured at the same temperature for both samples. We believe this effect to be due to the enhanced strength of dissimilar interactions near the core of A_2B_2 induced by the star branch point. We further show, by incorporating a simple model calculation due to Maurer et al. into the FH theory, that the difference in T_{ODT} is consistent with the degree of chain stretching observed experimentally.

For future work, we propose to improve the simple model we have used by performing a more rigorous calculation using the self-consistent one loop approach of Olvera de la Cruz and Barrat−Fredrickson.[9,10] This will allow the degree of non-Gaussian stretching and the consequent shift in T_{ODT} to be calculated from first principles. Parallel to this, it would also be interesting to address the problem using computer simulations similar to those in ref 8. We hope our study will stimulate other workers in the field to carry out further research in this direction.

Acknowledgment. D.M.A.B. acknowledges Dr. M. G. Brereton for helpful discussions on theoretical aspects of the work. I.W.H. acknowledges CLRC Daresbury Laboratories for the award of X-ray beamtime at the SRS and thanks Dr. B. U. Komanschek for assistance with the SAXS experiments. M.M., J.B.A., and R.N.Y. thank Professor N. Hadjichristidis and Dr. S. Pispas for the light scattering measurements on u-A_2B_2 and Dr. L. J. Fetters for triple detector SEC measurements on m-AB and m-A_2B_2.

References and Notes

(1) Iatrou, H.; Hadjichristidis, N. *Macromolecules* **1993**, *26*, 2479.
(2) Quirk, R. P.; Yoo, T.; Lee, B. J. *J. Macromol. Sci.- Pure Appl. Chem.* **1994**, *A31*, 911.
(3) Tsitsilianis, C.; Boulgaris, D. *J. Macromol. Sci., Pure Appl. Chem.* **1995**, *A32*, 569.
(4) Allgaier, J.; Young, R. N.; Efstratiadis, V.; Hadjichristidis, N. *Macromolecules* **1996**, *29*, 1794.
(5) Olvera de la Cruz, M.; Sanchez, I. C. *Macromolecules* **1986**, *19*, 2501.
(6) Fredrickson, G. H.; Helfand, E. *J. Chem. Phys.* **1987**, *87*, 697.
(7) Almdal, K.; Rosedale, J. H.; Bates, F. S.; Wignall, G. D.; Fredrickson, G. H. *Phys. Rev. Lett.* **1990**, *65*, 1112.
(8) Fried, H.; Binder, K. *J. Chem. Phys.* **1991**, *94*, 8349.
(9) Olvera de la Cruz, M. *Phys. Rev. Lett.* **1991**, *67*, 85.
(10) Barrat, J.-L.; Fredrickson, G. H. *J. Chem. Phys.* **1991**, *95*, 1281.
(11) Beyer, F. L.; Gido, S. P.; Poulos, Y.; Avgeropoulos, A.; Hadjichristidis, N. *Macromolecules* **1997**, *30*, 2373.
(12) Turner, C. M.; Sheller, N. B.; Foster, M. D.; Lee, B.; Corona-Galvan, S.; Quirk, R. P.; Annis, B.; Lin, J.-S. *Macromolecules* **1998**, *31*, 4372.
(13) Maurer, W. W.; Bates, F. S.; Lodge, T. P.; Almdal, K.; Mortensen, K.; Fredrickson, G. H. *J. Chem. Phys.* **1998**, *108*, 2989.
(14) Tselikas, Y.; Hadjichristidis, N.; Lescanec, R. L.; Honeker, C. C.; Wohlgemuth, M.; Thomas, E. L. *Macromolecules* **1996**, *29*, 3390.
(15) Bates, F. S.; Rosedale, J. H.; Fredrickson, G. H. *J. Chem. Phys.* **1990**, *92*, 6255.
(16) Rosedale, J. H.; Bates, F. S. *Macromolecules* **1990**, *23*, 2329.
(17) Bras, W.; Derbyshire, G. E.; Ryan, A. J.; Mant, G. R.; Felton, A.; Lewis, R. A.; Hall, C. J.; Greaves, G. N. *Nucl. Instrum. Methods Phys. Res.* **1993**, *A326*, 587.
(18) Bras, W.; Derbyshire, G. E.; Clarke, S.; Devine, A.; Komanschek, B. U.; Cooke, J.; Ryan, A. J. *J. Appl. Cryst.* **1995**, *28*, 26.
(19) Riise, B. L.; Fredrickson, G. H.; Larson, R. G.; Pearson, D. S. *Macromolecules* **1995**, *28*, 7653.
(20) Strobl, G. *The Physics of Polymers*, 2nd ed.; Springer-Verlag: Berlin, 1996; p 6.
(21) Hamley, I. W. *The Physics of Block Copolymers;* Oxford University Press: Oxford, U.K., 1998; pp 31−32.
(22) Leibler, L. *Macromolecules* **1980**, *13*, 1602.
(23) Dobrynin, A. V.; Erukhimovich, I. Ya. *Macromolecules* **1993**, *26*, 276.
(24) Read, D. J. *Macromolecules* **1998**, *31*, 899.
(25) Helfand, E.; Sapse, A. M. *J. Chem. Phys.* **1975**, *62*, 1327.
(26) Bates, F. S.; Schulz, M. F.; Khandpur, A. K.; Förster, S.; Rosedale, J. H.; Almdal, K.; Mortensen, K. *Faraday Discuss.* **1994**, *98*, 1.
(27) Olmsted, P. D.; Milner, S. T. *Macromolecules* **1998**, *31*, 4011.
(28) Fetters, L. J.; Lohse, D. J.; Richter, D.; Witten, T. A.; Zirkel, A. *Macromolecules* **1994**, *27*, 4639.
(29) Mori, K.; Hasegawa, H.; Hashimoto, T. *Polym. J.* **1985**, *17*, 799.
(30) Brazovskii, S. A. *Sov. Phys. JETP* **1975**, *41*, 85.
(31) Roan, J.-R.; Shakhnovich, E. I. *J. Chem. Phys.* **1998**, *109*, 7591.
(32) Dobrynin, A. V.; Yerukhimovich, I. Ya. *Polym. Sci. U.S.S.R.* **1991**, *33*, 1012.
(33) Strictly speaking, what Dobrynin−Erukhimovich calculate is the binodal for the isotropic to lamellar transition. However for $f = 0.5$, this coincides with the binodal of the ODT.
(34) Olvera de la Cruz, M. Private communication.

MA9904060